

A $\text{La}_{0.6}\text{Sr}_{0.4}\text{CoO}_{3-\delta}$ -based electrode with high durability for intermediate temperature solid oxide fuel cells

Fei Zhao, Ranran Peng, Changrong Xia *

Laboratory for Renewable Clean Energy, Department of Materials Science and Engineering, University of Science and Technology of China, Hefei, Anhui 230026, China

Received 20 January 2007; received in revised form 9 February 2007; accepted 1 March 2007

Available online 6 March 2007

Abstract

A highly stable electrode based on $\text{La}_{0.6}\text{Sr}_{0.4}\text{CoO}_{3-\delta}$ (LSC) was developed for intermediate temperature solid oxide fuel cells (IT-SOFCs). The electrode was prepared by impregnating LSC into a porous samaria-doped ceria (SDC, $\text{Sm}_{0.2}\text{Ce}_{0.8}\text{O}_{1.9}$) frame, which was deposited to an SDC electrolyte using screen-printing and co-firing techniques. The electrochemical properties of the composite electrode were investigated by impedance spectroscopy. High stability upon thermal cycle was demonstrated for this composite electrode although LSC and SDC have significant difference in thermal expansion. After 20 times of 500–800 °C thermal cycles and 10 times of room-temperature-to-800 °C thermal cycles, no increase in area specific resistance (ASR) was observed for such electrodes. In addition, improved performance was achieved with the impregnated composite electrode when compared with a conventional composite electrode prepared with a screen-printing technique.

© 2007 Elsevier Ltd. All rights reserved.

Keywords: A. Oxide; B. Electrochemical properties; C. Impedance spectroscopy; D. Thermal expansion

1. Introduction

Solid oxide fuel cells (SOFCs) are a forward looking technology for a highly efficient, environmental friendly power generation. An SOFC is a multilayer structure consisting at least of three layers; an electrolyte layer sandwiched between an anode and a cathode layer. These layers have to show a well adjusted thermal expansion behavior from room temperature to those operating temperatures to avoid cracking and delamination during SOFC operation and thermal cycling. Lanthanum cobaltite based perovskites such as $\text{La}_{0.6}\text{Sr}_{0.4}\text{CoO}_{3-\delta}$ (LSC) are attractive materials as cathodes for intermediate temperature (<800 °C) solid oxide fuel cells (IT-SOFCs) because they have higher catalytic activity in oxygen incorporation reaction, higher oxide ion conductivity, and higher electronic conductivity than lanthanum manganites, the classical cathodic materials for SOFCs [1,2]. However, the thermal expansion coefficient (TEC) of LSC (i.e. $\sim 23 \times 10^{-6} \text{ K}^{-1}$) is much higher than those of typical SOFC electrolytes, such as yttria-stabilized zirconia (YSZ) and doped ceria electrolytes ($11\text{--}12 \times 10^{-6} \text{ K}^{-1}$). TEC mismatch between the electrolyte and cathode will result in delamination at the cathode/electrolyte interface, and/or cracking of the electrolyte because of the stress developed upon heating and cooling [3]. To minimize the potential problems associated with TEC mismatch, efforts

* Corresponding author. Tel.: +86 551 3607475; fax: +86 551 3606689.

E-mail address: xiacr@ustc.edu.cn (C.R. Xia).

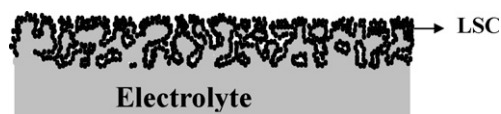


Fig. 1. Schematic diagram of the impregnated composite electrode.

have therefore been made to eliminate such TEC mismatch. For instance, by substituting Co with Fe and/or Ni in LSC, a low TEC ($14.8 \times 10^{-6} \text{ K}^{-1}$) was achieved for $\text{La}_{0.8}\text{Sr}_{0.2}\text{Co}_{0.2}\text{Fe}_{0.8}\text{O}_{3-\delta}$, which is still much higher (>20%) than that of those electrolytes [4]. Unfortunately, the decrease in thermal expansion is usually accompanied by the decline in conductivity for the perovskites $\text{La}_{1-x}\text{Sr}_x\text{Co}_{1-y}\text{Fe}_y\text{O}_{3-\delta}$ with low cobalt contents. Specifically at 600°C , the conductivity of $\text{La}_{0.8}\text{Sr}_{0.2}\text{Co}_{0.2}\text{Fe}_{0.8}\text{O}_{3-\delta}$ is only 77 S cm^{-1} whereas the conductivity is 1689 S cm^{-1} for $\text{La}_{0.8}\text{Sr}_{0.2}\text{CoO}_{3-\delta}$, and 2035 S cm^{-1} for $\text{La}_{0.6}\text{Sr}_{0.4}\text{CoO}_{3-\delta}$ [4]. In general, a highest possible conductivity is desired to minimize the ohmic losses of the electrode. In another example, the electrolyte was incorporated into LSC to form a composite cathode [5,6]. Theoretically, TEC of the composite cathode is smaller than that of LSC, but it is still larger than that of the electrolyte.

In addition, a new structure was proposed to modify the TEC mismatch. Shown in Fig. 1 is the schematic diagram of this structure in which the cathode consists of two continuous parts. One part is so-called cathode frame, which is porous and combined to the electrolyte. The cathode frame has a rigid connection with the electrolyte substrate and is made of the same material as the substrate. The other part is cobaltite based perovskite particles embedded in the frame and combined to current collecting materials. This structure was primarily reported for $\text{La}_{1-x}\text{Sr}_x\text{MnO}_{3-\delta}$ (LSM) based composite cathodes that were prepared with an ion-impregnation technique [7,8]. TEC decrease as an effect of this structure was firstly observed with a LSC–YSZ cathode by Huang et al. [9]. For example, TEC as low as $12.6 \times 10^{-6} \text{ K}^{-1}$ was observed for a YSZ frame with 55 wt.% LSC. However, performance losses with time were observed for the reported LSC–YSZ system. And the degradation was likely due to the formation of insulating phases, such as SrZrO_3 [9].

In this work, cathodes as shown in Fig. 1 were developed with samaria-doped ceria (SDC, $\text{Sm}_{0.2}\text{Ce}_{0.8}\text{O}_{1.9}$) as the electrolyte frame and LSC as the embedded component. Unlike YSZ, doped ceria is chemically stable with LSC at the operation temperature, and is often used as an interlayer for YSZ electrolyte based SOFC. Strong bonding is formed between the porous SDC frame and the dense electrolyte substrate by co-firing the two layers. The strong bonding makes the porous cathode frame and dense electrolyte substrate essentially one unified piece which will prevent delamination or cracking at the cathode/electrolyte interface during thermal cycle. Consequently, a high resistance to thermal shock is expected for this cathode. This was confirmed in this work with the degradation testing under abnormal conditions including thermal shock and thermal cycles.

2. Experimental

$\text{Sm}_{0.2}\text{Ce}_{0.8}\text{O}_{1.9}$ (SDC) powder used for substrates (electrolyte) was synthesized using an oxalate co-precipitation route and fired at 750°C for 2 h [10]. Fine SDC powder used for slurry was prepared using a glycine-nitrate method [11]. The powder was ball-milled with an ethyl cellulose binder and a terpeneol-based solvent for 24 h to form an uniform SDC slurry. The impregnated composite electrodes were prepared via a three-step process including substrate formation, frame coating and LSC impregnation. Firstly, SDC substrates were prepared by dry-pressing SDC powder at 300 MPa. Secondly, the slurry was applied to both sides of the green SDC substrates to fabricate symmetric cells with a screen-printing technique. The substrates with the printed bi-layers were subsequently dried and co-fired in air at 1350°C for 5 h to form dense SDC substrates supported porous SDC frames. The thicknesses for the porous SDC layer and dense SDC substrate were $\sim 50 \mu\text{m}$ and $\sim 0.8 \text{ mm}$, respectively, as measured with scanning electron microscopy (SEM). The area of the SDC frame was $\sim 1.2 \text{ cm}^2$. And finally, $\text{La}_{0.6}\text{Sr}_{0.4}\text{CoO}_{3-\delta}$ was imbedded to the frame with an ion impregnation technique. To do this, $\text{La}_{0.6}\text{Sr}_{0.4}\text{Co}(\text{NO}_3)_x$ nitrate solution was prepared by dissolving $\text{La}(\text{NO}_3)_3 \cdot 6\text{H}_2\text{O}$, $\text{Sr}(\text{NO}_3)_2$, and $\text{Co}(\text{NO}_3)_2 \cdot 6\text{H}_2\text{O}$ in distilled water at a molar ratio of La: Sr: Co = 0.6:0.4:1, followed by adding glycine with a molar ratio of glycine to nitrates of 0.5. A few drops of the nitrate solution were placed on top of the porous layer frame and then infiltrated into the SDC pores by capillary force. To introduce sufficient amounts of LSC, the impregnation was repeated several times. The impregnated salts were finally heated to 800°C for 2 h to remove the nitrate ions and organics, and form a perovskite LSC. The mass of the impregnated LSC before and after each impregnation cycle was measured to estimate the LSC loading. In this work, 10 mg LSC was impregnated into 1 cm^2 porous SDC frame ($50 \mu\text{m}$ thick) after 10

cycles. The final impregnated LSC–SDC electrode for measurement has a composition of 50 wt.% LSC and 50 wt.% porous SDC frame. For comparison, LSC–SDC composite (same weight fraction) electrode and pure LSC electrodes were prepared with the screen-printing technique and fired at 950 °C for 2 h.

The phase structure of the impregnated LSC electrode was investigated using X-ray diffraction (XRD, D/Maxra X diffractometer with Cu K α radiation). Microstructures were characterized using a JSM-6700F scanning electron microscope. Pt paste and Au wires were used for current collection in the symmetric electrodes. Two-probe measurements were conducted on the symmetric cells. Impedance spectra were measured on the symmetric cells under open-circuit conditions, with a frequency range from 0.01 Hz to 100 kHz and a 10 mV ac perturbation, using a ZAHNER IM6e electrochemical station.

3. Results and discussions

3.1. Stability upon thermal treatment

Shown in Fig. 2a is the area specific resistance (ASR) of the impregnated LSC–SDC electrode measured at 600 °C with ac impedance technique on a symmetric cell, where the SDC electrolyte was ~ 0.8 mm in thickness. ASR is typically used in the field of SOFC to quantify all resistances associated with the electrodes which occur at the gas/electrode interface, within the bulk of the electrode, or at the electrode/electrolyte interface [12]. The ASR data in this paper obtained in the Nyquist plot had been multiplied by 0.5 to account for the LSC–SDC electrodes. The impedance measurement was conducted under open-circuit conditions for a period of 30 days, in which two stages of thermal cycle were applied to the electrode. The first stage was performed at temperature between 500 and 800 °C with a heating and cooling rate of 5 °C/min. This stage proceeded with a fresh electrode, which was heated to 600 °C and held for 2 h to measure the first impedance. After the measurement, the temperature was raised to 800 °C and held for 30 min, followed by cooling to 500 °C and holding at 500 °C overnight. Finally the temperature was elevated to 600 °C for the next measurement. The thermal cycle was repeated 20 times and almost no increase in ASR was observed. On the contrary, a slight decrease in ASR was recorded. The ASR was $0.306 \Omega \text{ cm}^2$ for the first three measurements, and it dropped to $0.281 \Omega \text{ cm}^2$ after 20 thermal cycles. Therefore, this impregnated composite cathode showed high stability upon heating and cooling. The stability is further examined in the subsequent thermal shock test. The second stage was performed at temperatures between 800 °C and room temperature, at which the furnace was switched off to direct the shock test. The electrode temperature dropped to room temperature at a rate of up to 10 °C/min. The sample was further held at room temperature overnight and heated to 600 °C again for impedance measurement. As shown in Fig. 2a, ASR is $0.290 \pm 0.007 \Omega \text{ cm}^2$, and keeps almost constant in the period of 10 room-temperature-to-800 °C cycles.

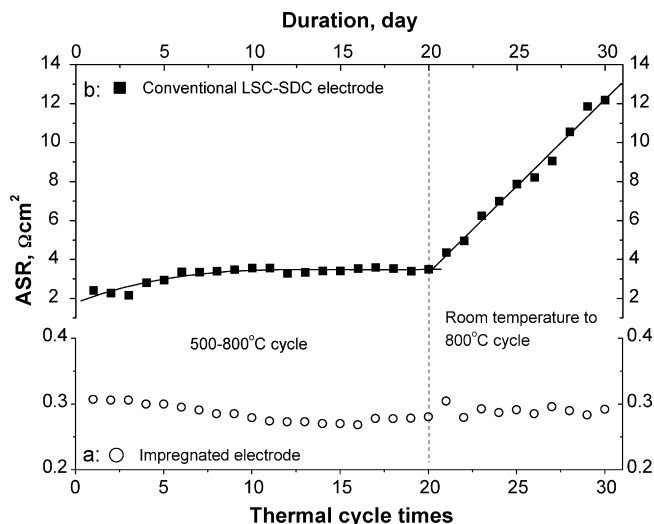


Fig. 2. ASR at 600 °C for (a) the impregnated electrode and (b) a conventional LSC–SDC electrode upon thermal cycles.

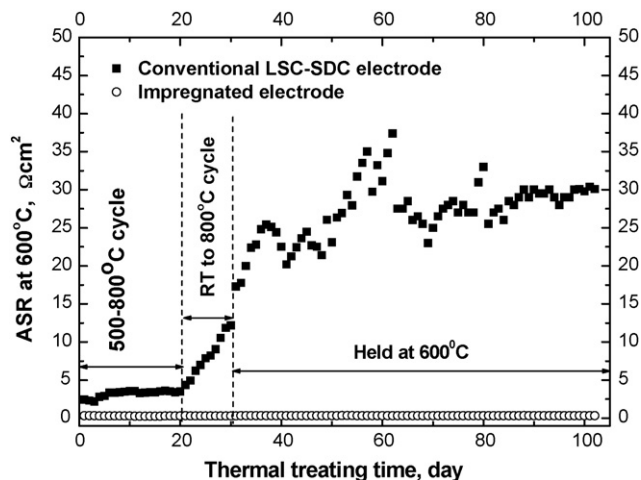


Fig. 3. ASR at 600 °C for the impregnated electrode and the conventional LSC–SDC electrode upon thermal treatment.

The advantages of this impregnated LSC–SDC electrode are distinctly illustrated by comparing the impregnated composite electrode with a conventional LSC–SDC (50 wt.% LSC + 50 wt.% SDC) composite electrode, which was prepared with conventional screen-printing technique. As shown in Fig. 2b, in the stage of the 500–800 °C thermal cycling tests, ASR of the conventional electrode increased from 2.42 to 3.50 $\Omega \text{ cm}^2$. Therefore, in the first stage of thermal cycle, ASR for the conventional LSC–SDC electrode increased about 45%, compared to a slight decrease in ASR for the impregnated electrode. The distinguished difference between the two electrodes was further observed at the second stage. ASR for the conventional electrode increased from 3.50 to 12.2 $\Omega \text{ cm}^2$, with an average increment of 0.93 $\Omega \text{ cm}^2$ per thermal cycle, while the ASR for the impregnated electrode kept almost constant.

The stability of the impregnated electrode upon thermal treatment is further shown in Fig. 3, where the electrode had been heat-treated for more than 2000 h. After 30 times thermal cycle, the electrode was held at 600 °C for more than 3 months. No obvious degradation was observed for the impregnated electrode whereas the conventional electrode was enormously unstable.

The high stability of this impregnated LSC–SDC electrode probably resulted from the special structure which consisted of two continuous parts (SDC phase and LSC phase). The major part is so-called electrode frame (SDC phase), which is porous and combined to the SDC electrolyte. Shown in Fig. 4a is the cross-sectional microstructure of the impregnated electrode, which is supported on an SDC electrolyte substrate. High-temperature sintering makes the electrode frame mechanically strong. The strong bonding makes the porous electrode frame and dense electrolyte substrate essentially one unified piece which will prevent delamination or cracking at the electrode/electrolyte interface during thermal cycles. Consequently, the high resistance to thermal shock is expected for such designed composite electrode, compared to the conventional LSC–SDC electrode which has a poor binding at the electrode/electrolyte interface shown in Fig. 4b.

3.2. Electrode activity of the impregnated composite electrode

It is encouraging that the impregnated LSC–SDC electrode showed not only superior thermal cycling performance but also enhanced electrode activity compared with the conventional LSC–SDC electrode. Comparing Fig. 2a with Fig. 2b it is clear that ASR of the impregnated electrode is about 1/8 of the conventional one, indicating that the impregnated electrode possessed much higher electrochemical performance. This advantage is further shown in Fig. 5, which presents ASR of the impregnated LSC–SDC electrode, the conventional LSC–SDC electrode, and a pure LSC electrode as a function of temperature. At 600 °C, ASR was only 0.29–0.31 $\Omega \text{ cm}^2$ for the impregnated electrode while it was 2.2–2.6 $\Omega \text{ cm}^2$ for the conventional electrode, and 10–14 $\Omega \text{ cm}^2$ for the pure LSC electrode. Clearly, ASR of the impregnated electrode is substantially lower than that of a single-phase LSC electrode (i.e. 1/5 to 1/10 of a conventional electrode) and is comparable to that of the best $\text{La}_{0.6}\text{Sr}_{0.4}\text{Co}_{0.2}\text{Fe}_{0.8}\text{O}_{3-\delta}$ -based composite systems with doped ceria as electrolytes [5,6]. It should be mentioned that the impregnated electrode had higher ASR than

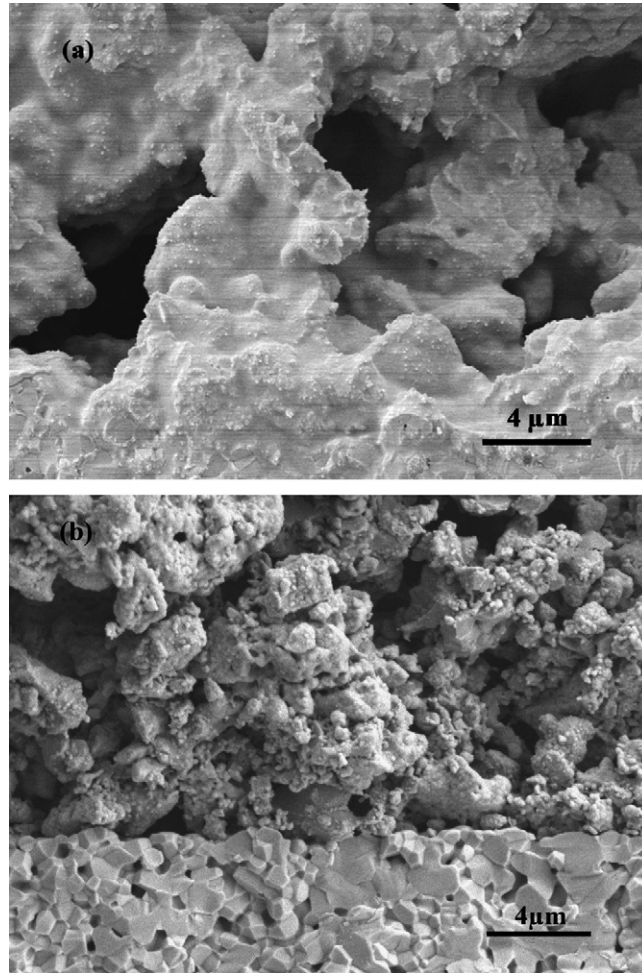


Fig. 4. Cross-sectional microstructure views of (a) the impregnated electrode, (b) the conventional LSC-SDC electrode.

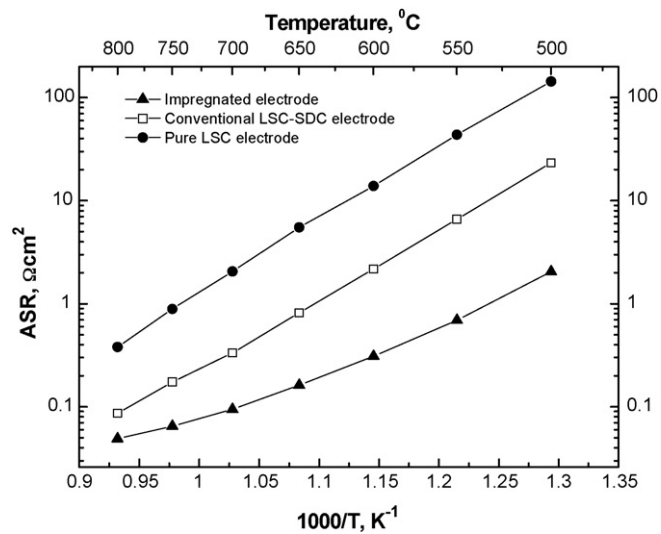


Fig. 5. Temperature dependence of ASR for the impregnated electrode, the conventional one, and a pure LSC electrode.

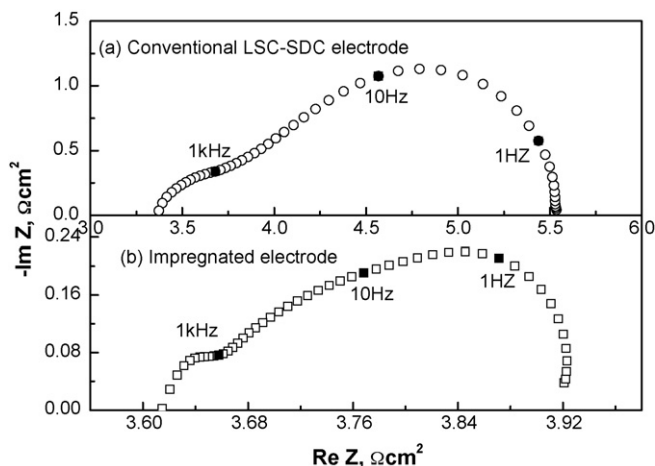


Fig. 6. Impedance spectra at 600 °C for the (a) conventional LSC–SDC electrode and (b) impregnated electrode.

BICUVOX and $\text{Ba}_{0.5}\text{Sr}_{0.5}\text{Co}_{0.8}\text{Fe}_{0.2}\text{O}_{3-\delta}$ (BSCF) based composites. The ASR was 0.055–0.071 $\Omega \text{ cm}^2$ at 600 °C for BSCF composites using SDC as the electrolyte [13,14]. However, the stability of these cathodes is still questionable. Shown in Fig. 6a and b are impedance spectra for the impregnated and conventional LSC–SDC electrodes. The two spectra are quite similar, implying the same oxygen reduction processes for the two electrodes.

The low ASR of the impregnated LSC–SDC electrode is also related to the microstructure of the composites. Fig. 5a shows that the electrode frame (SDC) was well-connected with SDC electrolyte, and the fine LSC particles coated the SDC frame. This well-connected structure makes a pathway for oxygen ion transport between the cathode (through the SDC frame) and the electrolyte (the SDC substrate) since SDC is an excellent oxide conductor. It should be noted that the pathway was not only built across the electrode/electrolyte “interface”, but also within the electrode. Therefore, the length of the triple phase boundaries (TPBs) was significantly extended. Consequently, cathodic activity is enhanced since oxygen reduction takes place only at or near the triple phase boundaries where oxygen ions can transport:



In a conventional cathode, it is difficult for oxygen ions to cross the interface. Furthermore, it is more difficult to travel within the cathode since oxygen ion pathway in the conventional cathode is built through the percolation of SDC

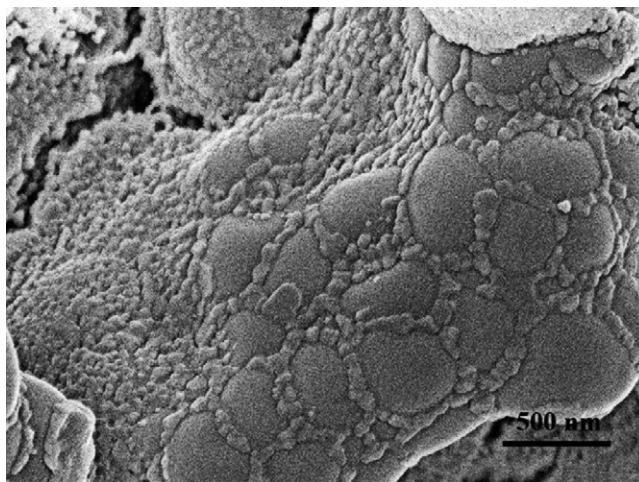


Fig. 7. Cross-sectional microstructure view of LSC particles coated on SDC grains.

particles. Therefore, the solid frame, which facilitates oxygen ion transport, may be one of the reasons for the reduced ASR of the impregnated electrode compared with the conventional composite electrode as well as the single phase LSC electrode, as shown in Fig. 5.

As shown in Fig. 4a, fine particles of LSC were coated on the surface of the frame grains and also embedded in the frame pores. SEM observation under higher magnification (Fig. 7) showed that the particles were ~ 50 nm in size, which was likely formed by decomposition of impregnated $\text{La}_{0.6}\text{Sr}_{0.4}\text{Co}(\text{NO}_3)_x$ nitrate solutions. This size is generally much smaller than that of particles in a conventional electrode. The latter has to be sintered at temperature higher than 900°C to obtain a reasonable bonding strength between the electrode and electrolyte. The small LSC particles as cathodic catalyst is believed to accelerate the rate of oxygen surface exchange, which is a critical step for oxygen reduction at the cathode, and also extend the length of TPBs. Therefore, small LSC particles should be another reason for the lower ASR of the impregnated electrode.

4. Conclusions

The present study has demonstrated that the $\text{La}_{0.6}\text{Sr}_{0.4}\text{Co}_{3-\delta}$ -impregnated electrode shows remarkable performance. The high resistance to thermal cycles and thermal shock has been achieved despite significant thermal expansion coefficient mismatch exists between $\text{La}_{0.6}\text{Sr}_{0.4}\text{Co}_{3-\delta}$ catalyst and $\text{Sm}_{0.2}\text{Ce}_{0.8}\text{O}_{1.9}$ electrolyte. In addition, very low area specific resistance has been achieved. These results imply that a reliable electrode with high thermal resistance and high performance has been developed for intermediate temperature solid oxide fuel cells.

Acknowledgements

This work was supported by the National Nature Science Foundation of China under award Nos. 50372066 and 50332040.

References

- [1] S.B. Adler, Chem. Rev. 104 (2004) 4791.
- [2] R.M. Ormerod, Chem. Soc. Rev. 32 (2003) 17.
- [3] N.Q. Minh, T. Takahashi, Science and Technology of Ceramic Fuel Cell, Elsevier, Amsterdam, Netherlands, 1995, p. 117.
- [4] A. Petric, P. Huang, F. Tietz, Solid State Ionics 135 (2000) 719.
- [5] V. Dusastre, J.A. Kilner, Solid State Ionics 126 (1999) 163.
- [6] E.P. Murray, M.J. Sever, S.A. Barnett, Solid State Ionics 148 (2002) 27.
- [7] Y. Huang, J.M. Vohs, R.J. Gorte, J. Electrochem. Soc. 152 (2005) 1347.
- [8] T.Z. Sholklapper, C. Lu, C.P. Jacobson, S.J. Visco, Electrochem. Solid-State Lett. 9 (2006) 376.
- [9] Y. Huang, K. Ahn, J.M. Vohs, R.J. Gorte, J. Electrochem. Soc. 151 (2004) 1592.
- [10] R.R. Peng, C.R. Xia, D.K. Peng, G.Y. Meng, Mater. Lett. 58 (2004) 604.
- [11] R.R. Peng, C.R. Xia, Q.X. Fu, G.Y. Meng, D.K. Peng, Mater. Lett. 56 (2002) 1043.
- [12] S.P. Jiang, Mater. Sci. Eng. A 418 (2006) 199.
- [13] Z.P. Shao, S.M. Haile, Nature 431 (2004) 170.
- [14] C.R. Xia, M.L. Liu, Adv. Mater. 14 (2002) 521.